Investigation of the Diffuser Flow Quality in an Icing Research Wind Tunnel

Harold E. Addy Jr.*
NASA Lewis Research Center, Cleveland, Ohio 44135
and
Theo G. Keith Jr.†
University of Toledo, Toledo, Ohio 43606

In this paper, the flow in the diffuser section of the Icing Research Tunnel at the NASA Lewis Research Center is both numerically and experimentally investigated. To accomplish the numerical portion of the work, an existing computer code is utilized. The code, known as PARC3D, is based on the Beam-Warming algorithm applied to the strong conservation law form of the complete Navier-Stokes equations. Following a brief description of the diffuser geometry, the measured flow characteristics are described. A brief discussion of the code work is also provided. The flow measurements show a highly nonuniform velocity profile across the diffuser exit with boundary-layer growth more prevalent near the centers of the walls rather than in the corners of the diffuser. Predicted velocity profiles at the centerline are similar to those measured; however, the code did not accurately predict the boundary-layer behavior near the corners.

Introduction

THE diffuser section of the Icing Research Tunnel (IRT) at the NASA Lewis Research Center has been used in the past to perform a limited amount of testing. However, measurements have shown that the flow quality is highly nonuniform and is unsuitable for many aerodynamic tests. That poor flow quality probably adversely affects the overall performance of the IRT, although the airflow in the test section appears to be well behaved. Because of that, it was decided that there was a need to better understand the peculiar flow characteristics in the diffuser of the IRT. That understanding may suggest methods that may be used to improve the flow quality. If this objective is realized, the diffuser can be more widely used as a second, larger, but lower speed, test section. Also, the study may help to improve the overall performance of the tunnel.

Diffusers are used to decelerate flows such that static pressure can be recovered, and in the case of wind tunnels, friction losses can be reduced. A number of studies have been performed to gather information on performance and characteristics of diffusers. However, much of the fundamental data in the literature is applicable to axisymmetric and/or two-dimensional diffusers. Little information exists for fully three-dimensional diffusers. The IRT diffuser, having four flat walls that all diverge at constant angles, is of this three-dimensional type.

As part of an ongoing IRT maintenance and upgrade program, a series of detailed flow measurements were planned for the tunnel to better establish its present flow characteristics. This flow measurement program allowed the opportunity to not only record information on three-dimensional diffusers but also to provide a base of experimental data with which to compare numerical diffuser flow simulations.

Numerical simulation techniques are increasingly being used to model and study internal flows. An existing computer code was used to model the flow in the diffuser of the IRT. This program is the PARC3D code, which utilizes the complete Navier-Stokes equations and can be applied to model a wide range of internal flows.

IRT Geometry and Measured Flow Characteristics

Icing Research Tunnel

The IRT, which was completed in 1944, is a closed-loop wind tunnel designed for test section airspeeds of up to 300 mph. A large refrigeration system allows the tunnel total temperature to be independently set as low as −20 °F. Air flows from the settling chamber through a 14.13:1.0 contraction ratio into the test section that is 20 ft long and has a rectangular cross section that is 6 ft high and 9 ft wide. The settling chamber and the contraction section are also rectangular in shape, as is the diffuser. A plan view of the tunnel is shown in Fig. 1. Throughout the paper, the inside wall of the diffuser is synonymous with the north wall. Similarly, the south wall of the diffuser and the outside wall are the same.

The portion of the IRT that forms the primary diffuser is bounded by locations marked 1 and 2 in Fig. 1. This portion is 81.5 ft long and consists of four flat, straight walls, each of which diverges from the centerline at an angle of 2.5 deg. The diffuser entrance is 6 ft high and 9 ft wide whereas the exit is 13.469 ft high and 16.469 ft wide. The expansion ratio of the diffuser is 4.11:1.0.

Flow Measurements

The locations marked 1 and 2 in Fig. 1 indicate where quantitative measurements of the flow were made in the IRT diffuser. At each location, local total temperatures and static and total pressures were measured using instrumentation rakes as shown in Figs. 2 and 3. These rakes were designed to minimize their effect on the flow and the measurements themselves.[1,2] The pressures from the instrumentation rakes were measured by individual transducers on an Electro-Scan Pressure System (ESP). This system employs oscillating quartz

Presented as Paper 89-0755 at the AIAA 27th Aerospace Sciences Meeting, Reno, NV, Jan. 9–12, 1989 and Paper 90-0488 at the AIAA 28th Aerospace Sciences Meeting, Reno, NV, Jan. 8–11, 1990; received May 30, 1990; revision received Nov. 15, 1990; accepted for publication Dec. 10, 1990.

*Aerospace Engineer, Icing and Cryogenics Technology Branch, Propulsion Systems Division, 21000 Brookpark Road. Member AIAA.

†Professor, Mechanical Engineering Department. Associate Fellow AIAA.

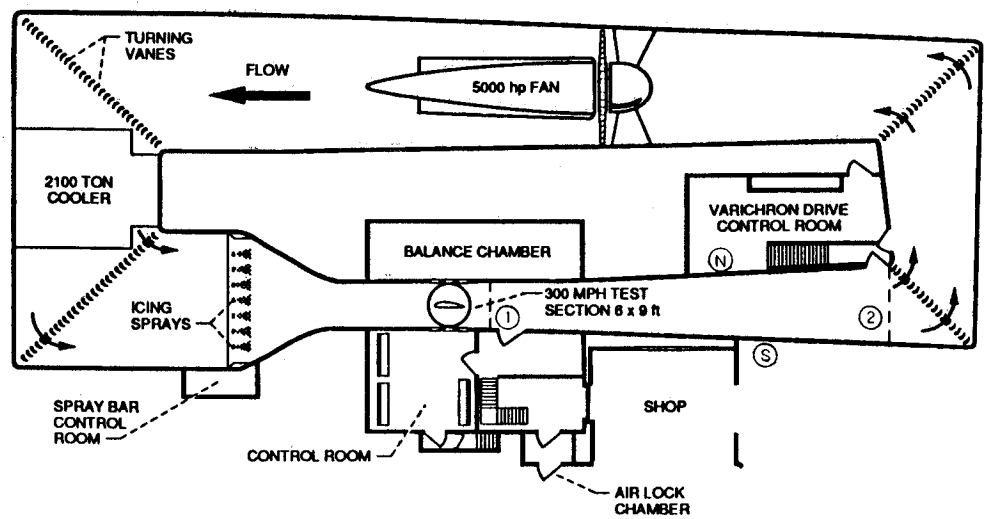

Fig. 1 NASA Lewis Icing Research Tunnel—plan view.

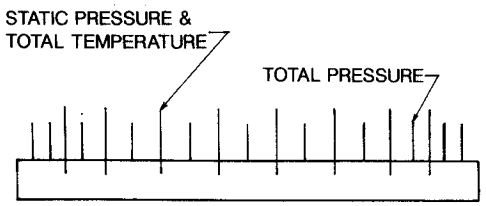

Fig. 2 Instrumentation rake—plan view

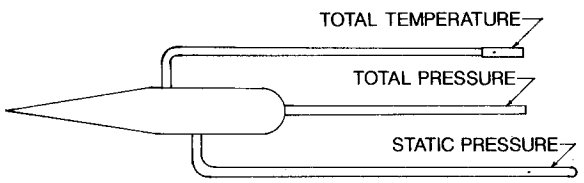

Fig. 3 Instrumentation rake—side view.

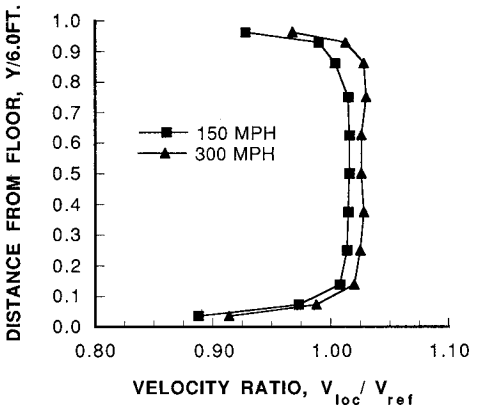

Fig. 4 Measured vertical velocity profiles at diffuser entrance.

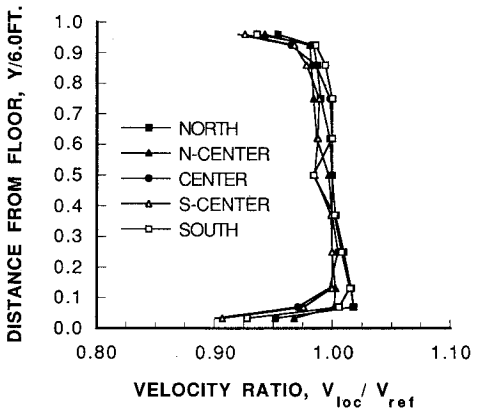

Fig. 5 Measured vertical velocity profiles across diffuser entrance, Vref = 200 mph.

crystals and is a secondary standard traceable to the National Institute of Standards Technology. Each transducer is of the differential type and was referenced to the tunnel total pressure as measured by the facility heated pitot-static tube. Both 1.0 psid (pounds per square in., differential) and 5.0 psid transducers were used in the tests. The 1.0 psid transducers have an accuracy of ±0.003 psi whereas the 5.0 psid transducers have an accuracy of ±0.007 psi. The tunnel total pressure was measured using a 15 psia ESP transducer having an accuracy of ±0.005 psi.

The local total temperatures were measured using aspirated, copper-constantan thermocouples that were referenced to a floating point thermocouple junction box. The temperature of the floating point junction box was monitored by a platinum resistance thermometer. For routine tunnel testing, the total temperature is monitored by 11 copper-constantan thermocouples that are mounted on the turning vanes located downstream of the refrigeration system and upstream of the contraction section of the tunnel. These thermocouples are also referenced to a floating point thermocouple junction block. The average of the temperatures read by these thermocouples was used to set the tunnel operating temperature. The overall accuracy of each individual temperature measurement is ±0.75 °F.

The measurements and calculations were nominalized to minimize the effects of small variations in tunnel conditions from test run to test run. Local pressure measurements were nominalized by the facility pitot-static tube pressure measurements, the local temperatures were nominalized by the average of the 11 facility total temperatures, and the local velocity calculations were nominalized by the velocity calculated from the facility pitot-static tube and the average facility temperature.

Measurements were taken at six tunnel airspeeds: 50, 100, 150, 200, 250, and 300 mph at an average tunnel temperature of 0 °F at the diffuser entrance. In an earlier study,[3] it was found that variation in the average tunnel operating temperature has no noticeable effect on the flow characteristics. The horizontally mounted instrumentation rake used in the diffuser section exit was much longer than any of the rakes used in the diffuser entrance, and it exhibited excessive vibration at the higher speeds; therefore, measurements were taken at only five tunnel airspeeds: 50, 100, 150, 200, and 228 mph (as measured by the facility pitot-static tube). Since tests using the vertically mounted instrumentation rake in the diffuser

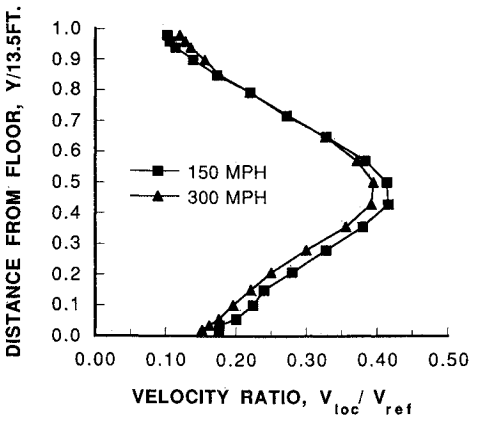

Fig. 6 Measured vertical velocity profiles at diffuser exit.

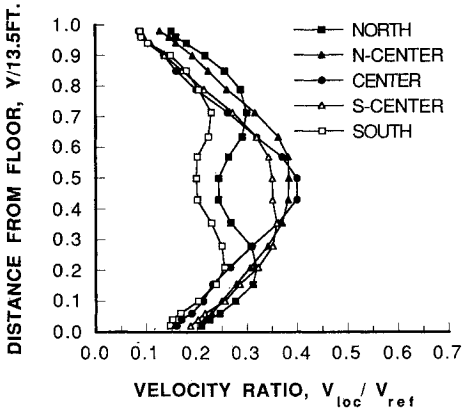

Fig. 7 Measured vertical velocity profiles across diffuser exit, Vref = 200 mph.

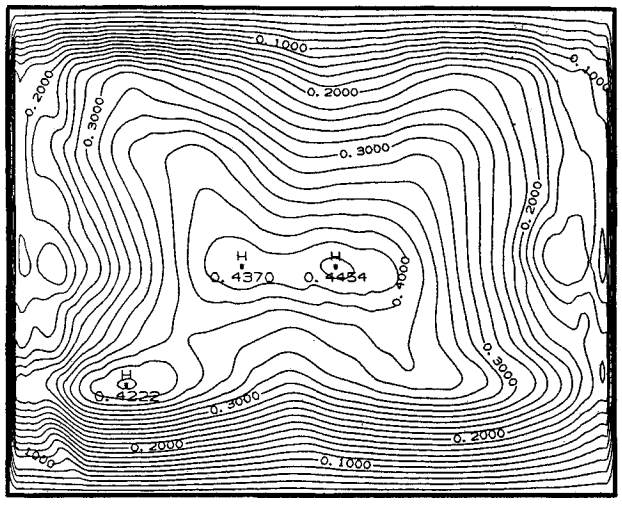

Fig. 8 Measured velocity contours at diffuser exit.

exit were scheduled at a later date, there was sufficient time to structurally stiffen this rake such that it could be used over the entire operating range of the tunnel.

Based on the measurements taken, the flow in the test section and the diffuser entrance appears to be well behaved. Figure 4 shows measured vertical velocity profiles at the centerline of the diffuser entrance for test section speeds of 150 and 300 mph. Figure 5 shows measured vertical velocity profiles in five equally spaced locations across the diffuser entrance for a test section speed of 200 mph. In each of these figures, the vertical location of the local measurement above the floor of the tunnel is plotted against the local value of the

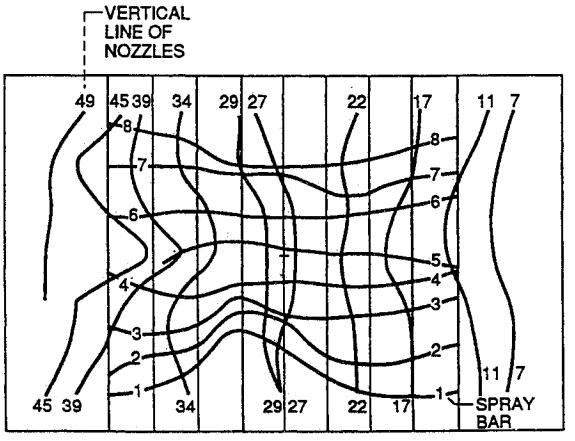

Fig. 9 Map of peak LWC in test section.

measurement that is nominalized by the tunnel reference value as measured by the facility pitot-static tube located in the test section. As may be seen, each of these profiles is relatively flat and uniform. Flow in the diffuser exit is markedly different from that measured in the diffuser inlet. Figure 6 shows measured vertical velocity profiles at the centerline of the diffuser exit for test section airspeeds of 150 and 300 mph. As can be seen, these profiles are nonuniform. Figure 7 shows measured vertical velocity profiles at five equally spaced locations across the diffuser exit for a test section airspeed of 200 mph. Not only are these profiles nonuniform, but adjacent profiles are dissimilar. The north and south profiles in Fig. 7 indicate that the flow is tending to migrate toward each of the four corners of the diffuser exit or, conversely, the boundary layers along the center of the walls are growing more rapidly than at the corners. The contour plot of measured local velocities at the diffuser exit at 150 mph is shown in Fig. 8 and also demonstrates this tendency in the flow.

It is interesting to also note that a similarity exists between the measured airflow velocity contour plot in the diffuser exit and a test section map of peak liquid water content (LWC) from each spray bar in the system.[4] Figure 9 shows such a map of this peak LWC. This map was established by accreting ice on 2-in. diam vertical bars mounted in the test section. Each of the eight horizontally mounted spray bars located in the settling chamber of the tunnel were individually operated. The horizontal lines numbered 1–8 in the map indicate the line of maximum ice accretion on each of the vertical bars in the test section. The numbered vertical lines in the map indicate the maximum ice accretion when a single vertical column of nozzles was operated. At present, it is not understood why the distribution of water droplets is uneven and unlike the velocity distibution that is quite uniform. The relatively short contraction section of the tunnel has been suggested as a possible cause in that the more dense water droplets may not be able to follow the path of the airflow. Also, the higher ratio of primary to secondary velocity of the air in the test section may be overshadowing airflow characteristics that show up in the diffuser. Thus far, efforts to redistribute the icing cloud as evenly as possible across the test section by repositioning the spray nozzles have met with limited success, and these peculiarities in the flow indicte the need for further aerodynamic investigation and suggest that these flow characteristics may not be limited to the diffuser.

PARC3D Computer Code

An existing computer code[5] was used to simulate the flow in the IRT. This code is known as PARC3D. It is based on the complete Navier-Stokes equations written in strong conservation law form. The code uses the Beam and Warming approximate factorization algorithm[6] to solve a set of finite-difference equations that were produced by central differencing the Navier-Stokes equations on a regular grid. The

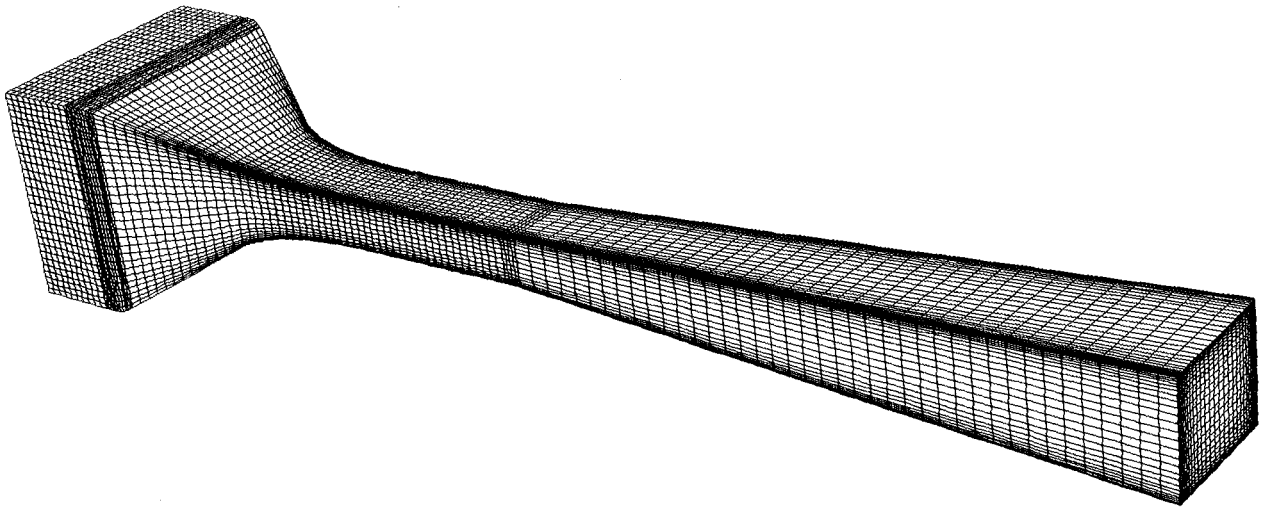

Fig. 10 PARC3D mesh for settling chamber through diffuser of the IRT.

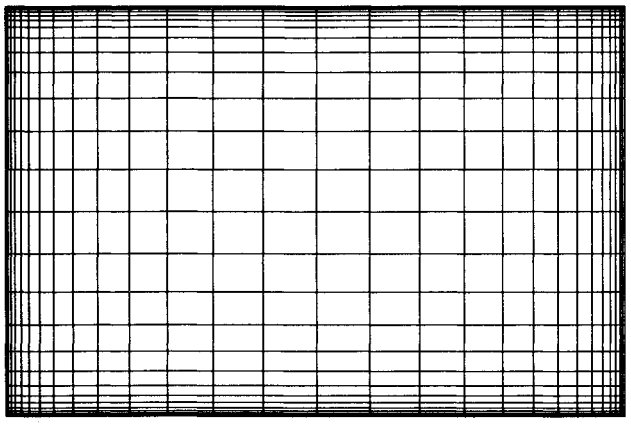

Fig. 11 Cross section of mesh used in the PARC3D code.

code calculates flow characteristics based on a specified boundary geometry and the corresponding flow conditions on these boundaries. A wide range of geometries and boundary conditions may be specified. The flow can be either inviscid or viscous. If viscous, it can be treated as either laminar or turbulent. The turbulence model used is the relatively simple algebraic model of Baldwin and Lomax.[7] In this study, both laminar flow and turbulent flow simulations were run because it was not clear that the flow in the tunnel should be considered turbulent for this computation and because it was felt that the Baldwin and Lomax turbulence model may overshadow some flow characteristics that might show up in the laminar simulation.

The PARC3D code requires the following input: a grid, initial and boundary conditions, and program execution controls. The initial condition, which may also be regarded as an initial solution, does not need to be an accurate one because only steady-state results, which are obtained by an asymptotic time march, are of interest. Thus, only a rough, approximate solution is required to get the processing started.

The primary boundary conditions used for the IRT flow simulation runs were four no-slip, adiabatic walls and subsonic inlet and outlet flows. Uniform distributions of total pressure and temperature were specified on the inflow boundary. Measurements made in the diffuser entrance indicate that this ia a good approximation of actual conditions in this portion of the tunnel. At the exit to the diffuser, a uniform static pressure, corresponding to a particular tunnel airspeed, was prescribed. The program controls allow the user limited control over program execution such as limiting the total number of iterations, maximum time-step size, tabular output, and so forth.

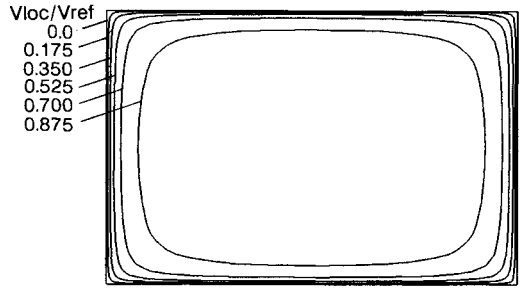

Fig. 12 Predicted velocity contours at diffuser entrance; laminar flow, Vref = 150 mph.

The grid configuration for this investigation is shown in Fig. 10. This grid models the entire main leg of the IRT, including the settling chamber, the contraction section, the test section, and the diffuser. As shown in Fig. 11, the grid also represents a full cross section of the tunnel, rather than a one-quarter or one-half section. This was done even though the main leg of the IRT is geometrically symmetric in both the horizontal and vertical planes to allow for subsequent modeling of wall obstacles, such as facility pitot-static tubes and handrails, or of flow effects, such as balance chamber vents and heated windows.

The grid-generation scheme developed for this work allowed for grid packing near the walls. This was desired to resolve the larger gradients in the flow that were anticipated in these regions. The grids generated had a cross section of 29 points by 29 points and included 55 points in the axial direction. It is recognized that this grid is a bit coarse and may not have sufficient grid lines within the wall layers. However, it was deemed an adequate starting structure for this problem.

Results and Discussion

For this discussion, the results from both a laminar and a turbulent flow simulation will be presented. Both cases are for a test section velocity of 150 mph. Figure 12 shows predicted velocity contours at the diffuser entrance for the laminar flow case. The contours are regular and symmetric around the tunnel walls, depicting a uniformly varying velocity profile. Predicted velocity contours at the exit of the diffuser for this case are presented in Fig. 13. The flow again behaves here, with the velocity uniformly varying across the tunnel. Regions of flow separation or backflow are shown in each of the four corners.

Figure 14 presents predicted velocity contours at the diffuser entrance for the turbulent flow simulation. These contours are also regular and symmetric. Figure 15 shows pre-

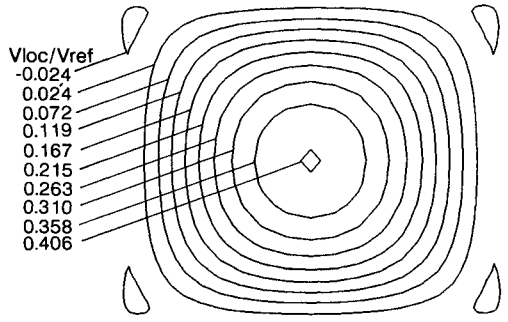

Fig. 13 Predicted velocity contours at diffuser exit; laminar flow, Vref = 150 mph.

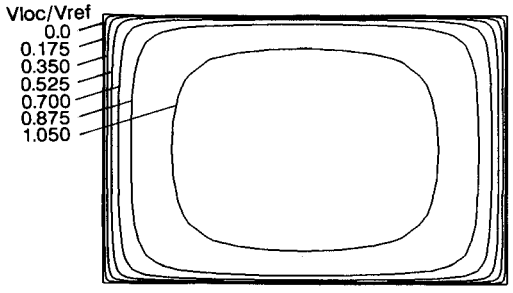

Fig. 14 Predicted velocity contours at diffuser entrance; turbulent flow, Vref = 150 mph.

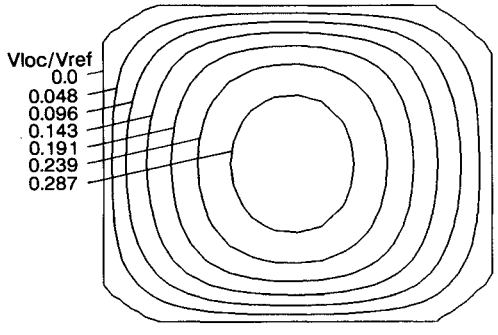

Fig. 15 Predicted velocity contours at diffuser exit; turbulent flow, Vref = 150 mph.

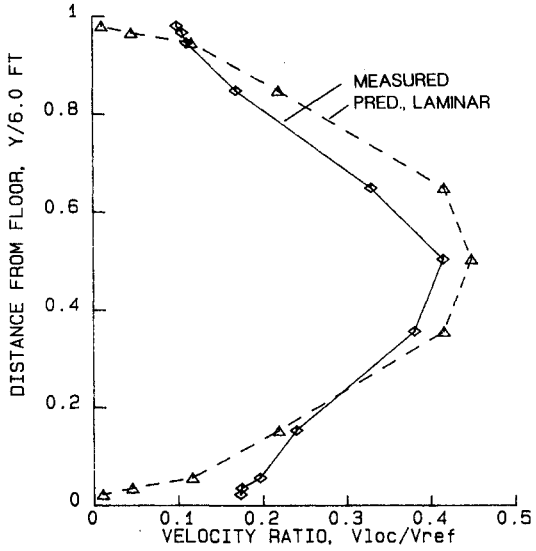

Fig. 16 Comparison of velocity profiles at diffuser exit at 150 mph; measured and predicted by PARC3D.

dicted velocity contours at the diffuser exit. The flow pattern is similar to the previous, laminar flow case; however, less separation or backflow is predicted in each of the four corners of the cross section.

In contrasting the measured velocity profiles with those from the computed results, several features should be mentioned. First, the predicted boundary-layer thichnesses of 9% of tunnel height for the laminar simulation and 11% for the turbulent simulation are in good agreement with the measured results of approximately 10% of the tunnel height. Furthermore, in contrasting the shapes of the velocity profiles at the diffuser exit as shown in Fig. 16, it is evident that the extended grid, laminar flow case most closely resembles the shape of the measured profile.

Concluding Remarks

The aerodynamic measurements made in the diffuser of the IRT indicate a degree of complexity heretofore unanticipated. The tendency of the boundary layers on the walls of the diffuser to grow more rapidly than in the corners was unexpected, and the source of this behavior is unknown; however, it does seem to allow the flow in the corners to be energized, which helps retard the flow separation anticipated by the computer code in these areas.

One of the primary purposes of this work was to numerically simulate the flow in the diffuser section of the IRT. It was found that the PARC3D computer code predicted centerline velocity profiles with reasonable accuracy; however, it did not predict the flow characteristics in the corners of the diffuser very closely. Several steps may be taken to improve this agreement:

1) Further refinement of the grid structure is warranted. In particular, the wall layers require more grid points than were used in the current study.

2) An investigation needs to be performed to ascertain that the predicted results are nongrid dependent.

3) Downstream turning vane effects need to be incorporated into the simulation. These will help to generate the asymmetry conditions seen in the measured flowfield values but not present in the predictions.

4) Flow angularity measurements need to be made in the contraction section and/or the test section to verify that the uniform inflow boundary condition is valid.

Besides the above, it is recommended that the numerical simulation of the IRT include the following: 1) numerical solution of the energy equation so that tunnel temperature distributions could also be predicted and contrasted to measured values, and 2) a particle trajectory code to predict the pattern of the icing cloud spray.

References

[1]Krause, L. N., and Gettelman, C. C., "Effect of Interaction Among Probes, Supports, Duct Walls, And Jet Boundaries on Pressure Measurements in Ducts and Jets," *ISA Proceedings*, Vol. 7, Paper 52-12-2, 1952, pp. 138–141.

[2]Gettelman, C. C., and Krause, L. N., "Considerations Entering into the Selection of Probes for Pressure Measurements in Jet Engines," *ISA Proceedings*, Vol. 7, Paper 52-12-1, 1952, pp. 134–137.

[3]Soeder, R. H., and Andracchio, C. R., "NASA Lewis Icing Research Tunnel User Manual," NASA Tech. Memo. 102319, June 1990.

[4]Ide, R., "Liquid Water Content and Droplet Size Calibration of the NASA-Lewis Icing Research Tunnel," AIAA Paper 90-0669, Jan. 1990.

[5]Cooper, G. K., and Sirbaugh, J. R., "The PARC Distinction: A Practical Flow Simulator," AIAA Paper 90-2002, July 1990.

[6]Beam, R., and Warming, R. F., "An Implicit Finite-Difference Algorithm for Hyperbolic Systems in Conservation-Law Form," *Journal of Computational Physics*, Vol. 22, No. 1, Sept. 1976, pp. 87–110.

[7]Baldwin, B. S., and Lomax, H. "Thin Layer Approximation and Algebraic Model for Separated Turbulent Flows," AIAA 78-257, Jan. 1978.